Atmos. Chem. Phys. Discuss., 11, 7291–7319, 2011
www.atmos-chem-phys-discuss.net/11/7291/2011/
doi:10.5194/acpd-11-7291-2011

Atmospheric Chemistry and Physics Discussions

Satellite-based evidence of wavelength-dependent aerosol absorption in biomass burning smoke inferred from ozone monitoring instrument

H. Jethva[1] **and O. Torres**[2]

[1]Department of Atmospheric & Planetary Sciences, Hampton University, Hampton, VA 23668, USA
[2]NASA Goddard Space Flight Center, Greenbelt, MD, 20771, USA

Received: 15 February 2011 – Accepted: 16 February 2011 – Published: 2 March 2011

Correspondence to: H. Jethva (hiren.jethva@hamptonu.edu)

Published by Copernicus Publications on behalf of the European Geosciences Union.

Abstract

We provide satellite-based evidence of the spectral dependence of absorption in biomass burning aerosols over South America using near-UV measurements made by Ozone Monitoring Instrument (OMI) during 2005–2007. Currently, OMAERUV aerosol algorithm characterizes carbonaceous aerosol as "gray" aerosol, meaning no wavelength dependence in aerosol absorption. With this assumption, OMI-derived aerosol optical depth (AOD) is found to be over-estimated significantly compared to that of AERONET at several sites during intense biomass burning events (August–September). The assumption on height of aerosols and other parameters seem to be reasonable and unable to explain large discrepancy in the retrieval. The specific ground-based studies have revealed strong spectral dependence in aerosol absorption in the near-UV region that indicates the presence of organic carbon. A new set of OMI aerosol retrieval with assumed wavelength-dependent aerosol absorption in the near-UV region (Absorption Angstrom Exponent $\lambda^{-2.5\,\text{to}\,-3.0}$) provided much improved retrieval of AOD with significantly reduced bias. Also, the new retrieval of single-scattering albedo is in better agreement with those of AERONET within the uncertainties ($\Delta\omega = \pm 0.03$). The new smoke aerosol model was also found to be valid over the biomass burning region of central Africa and northern India. Together with suggesting vast improvement in the retrieval of aerosol properties from OMI, present study demonstrates the near-UV capabilities of OMI in separating aerosols containing organics from pure black carbon through OMI-AERONET integrated measurements.

1 Introduction

Biomass burning is a major source of particulate matter in the atmosphere over several regions of the world, the tropics in particular. The biomass burning of forests and agriculture in the tropics contributes to increase in aerosol optical depth, AOD (Venkataraman et al., 2005). For instance, the Amazonia region in South America accounts for about one third of total biomass burning activities in the tropics. These

ACPD
11, 7291–7319, 2011

events emit huge amount of aerosols with dominant carbonaceous compounds such as black carbon (BC) or soot, and organic carbon (OC) also referred to as brown carbon. While BC is the most efficient known absorber of light in atmosphere, the OC component of biomass burning has been characterized by several studies in the recent time. Though OC is found to be a weaker absorber of light in the visible spectrum compared to the strongly absorbing BC, the distinct spectral absorption makes it an important species in the UV part of spectrum. The results of GCM experiments on impact of smoke on circulation show that the strongly absorbing smoke aerosols can stabilize the lower troposphere, yielding weaker convergence and suppressed monsoon activities over the aerosol-laden region (Zhang et al., 2009). Because of their radiative impacts on the Earth's radiation budget and climate, carbonaceous aerosols have received a great amount of attention by the atmospheric science community. Multi-year long data records on aerosol optical depth of carbonaceous aerosols collected from several satellite borne sensors like Total Ozone Measuring Instrument (TOMS) (Torres et al., 2002), Moderate-resolution Imaging Spectroradiometer (MODIS) (Kaufman et al., 1997; Remer et al., 2005; Levy et al., 2007), Multiangle Imaging Spectroradiometer (MISR) (Kahn et al., 2005), and Ozone Monitoring Instrument (OMI) (Torres et al., 2007; Ahn et al., 2008) are currently available. The aerosol physical and optical properties and associated variability over the Amazon basin have been studied and reported by several investigations using ground based (Eck et al., 1998; Martins et al., 1998; Reid et al., 1998) as well as satellite observations (Koren et al., 2008; Torres et al., 2010). This region is one of the prominent regions of intense biomass burning during August–September months with some year-to-year temporal variability (Torres et al., 2010). In addition to aerosol data collected during specific field campaigns, the sunphotometer installed as a part of AERONET at several sites in the region also provide remotely sensed high quality data on aerosol optical properties (Holben et al., 1998). Because of the known sensitivity of near-UV observations to aerosol absorption (Torres et al., 1998, 2007), satellite observations by the TOMS and OMI sensors are specially suited for the detection and characterization of BC and OC containing aerosol particles.

ACPD
11, 7291–7319, 2011

Figure 1 shows the September 2007 monthly mean spatial distribution of the atmospheric aerosol load over South America in terms of the Aerosol Index (AI) derived from OMI observations. AI is derived from the change in the spectral dependence of the back-scattered UV radiance induced by aerosols relative to the Rayleigh scattering between 354 and 388 nm (Torres et al., 2007). It is a useful qualitative indicator of the presence of absorbing and elevated aerosols, such as biomass burning plumes and dust aerosols. A cup-shape spatial distribution of AI shows high values over the central part of SA indicating the presence of absorbing aerosols, and relatively lower AI values towards the south.

In addition to the AI, OMI-measured near-UV radiances at 354 and 388 nm are used as input to an inversion algorithm to derive AOD and single scattering albedo (SSA) at 388 nm. The OMI near-UV inversion algorithm (OMAERUV) is one of two operational OMI aerosol products. Another retrieval scheme that uses a multi-spectral fit (OMAER0) is also available (Torres et al., 2007). As with any aerosol inversion procedure retrievals are derived based on certain assumptions made in the algorithm; therefore, their assessment against accurate ground-based measurements is necessary. In the present study, we evaluate the OMAERUV retrieved aerosol parameters against those of AERONET over selected stations in South America's biomass burning region (see Fig. 1). Section 2 briefly describes the OMI aerosol inversion procedure and dataset used in the analysis. The results and interpretation of the OMAERUV-AERONET comparison are presented in Sect. 3. Section 4 discusses the findings of the ground-based studies on the spectral aerosol absorption. A new set of OMAERUV retrieval based on theoretical calculations and ground-based observations is presented and discussed in Sect. 5. The results of the present study are concluded in Sect. 6.

2 A brief description of OMI aerosol inversion and dataset

The UV part of the solar spectrum has distinct and unique advantages for the characterization of aerosol properties. Most surfaces, including visibly bright desert appear

ACPD
11, 7291–7319, 2011

dark due to low surface reflectivity at UV wavelengths. This is a favorable condition as it leads to less surface contamination in total signal at top-of-atmosphere. Secondly, multiple interactions of Rayleigh-scattered radiation with aerosols provide an opportunity to infer the aerosol absorption under clear as well as cloudy conditions. OMI is a successor of the TOMS series of instruments with hyper-spectral imaging capability at higher spatial resolution than other UV-capable sensors [GOME, GOME-2 SCIamachy]. Along with qualitative and quantitative information on aerosols, OMI also derives total column ozone and its vertical distribution, total column amounts of the trace gases NO_2, SO_2, HCHO, BrO, and OClO (Levelt et al., 2006).

The OMI aerosol index (similar to TOMS AI) is directly derived quantity using observed radiances at 354 and 388 nm. OMI takes this advantage of greater sensitivity of radiances measured at the top-of-atmosphere in the near-UV region to the varying load and types of aerosols to derive extinction aerosol optical depth, SSA at 388 nm, and absorption AOD using an inversion procedure. Currently, OMI assumes a set of "gray" aerosol model, meaning wavelength-independent absorption, to derive aerosol properties over the biomass burning regions. The assumed particle size distributions of these models were derived from the multi-year AERONET measurements over the major biomass burning regions of the world (Torres et al., 2007). The wavelength independent absorption is a good proxy for the aerosols dominated by black carbon (BC). The top-of-atmosphere radiances are generated at 354 and 388 nm wavelengths for a set of given geometry, aerosol profile (normal distribution with peak at 3 km), six values of aerosol optical depth and seven aerosol model as characterized by single-scattering albedo at 388 nm. Thus, the measured radiance at two UV wavelengths are associated with a set of aerosol optical depth and single-scattering albedo values. The retrieved values of AOD and SSA at 388 nm are converted to 354 and 500 nm using the spectral dependence associated with the assumed aerosol model.

The OMAERUV algorithm uses observed Lambertian Equivalent Reflectivity (LER) at 388 nm (R_{388}) and aerosol index as the combined criteria to assign a flag number to each retrieval which suggests the quality of aerosol retrieval. As per the current quality

ACPD
11, 7291–7319, 2011

flag scheme, the retrieval with flag 0 (lower R_{388}) are considered to be reliable in AOD and AAOD, whereas the retrieval with flag 1 ($R_{388} < 0.30$ and AI > 1) are expected to be contaminated by minimum clouds and therefore AOD is not reliable. However, AAOD which is only sensitive to absorption is considered to be still reliable. A more detailed description of OMI UV aerosol algorithm is presented in Torres et al. (2007). We use OMI Level 2 OMAERUV Collection 3 aerosol product, including aerosol optical depth at 388 nm, UV aerosol index, single-scattering albedo, and radiance at these channels in our analysis. The instrumental footprint of these dataset is $13 \times 24\,\mathrm{km}^{2\,\mathrm{at\,nadir}}$. We have considered aerosol retrieval with flag 0, and 1 in comparison against AERONET measurements.

The validation of OMI aerosol products is an ongoing activity. Torres et al. (2007) compared the OMI-derived AOD with that of AERONET direct sun measurements and found that under minimum cloud interference the OMAERUV-AERONET comparison was reasonable. This paper also compared OMAERUV aerosol absorption product with AERONET-retrieved single-scattering albedo and showed that two independently derived quantities agree quite well within the uncertainty (±0.03). Ahn et al. (2008) have compared the OMI-derived AOD with that of MODIS and MISR and found that in spite of a positive offset of 0.15, OMI retrieval show high degree of correlation with the two independently derived quantities. Also, OMI is able to capture the seasonal annual cycles of aerosols over major biomass burning and mineral dust emission sources. Given the large OMI footprint, sub-pixel cloud contamination is the most important source of uncertainty of the OMAERUV aerosol products.

The AErosol RObotic NETwork (AERONET) is a ground-based federated network of Cimel sunphotometer that measures the extinction aerosol optical depth at seven wavelengths (340, 380, 440, 500, 670, 870, 1020 nm) from the direct sun measurements over worldwide locations (Holben et al., 1998). The AOD measurements are accurate to within ±0.01. AERONET also retrieves aerosol optical and particle size distribution properties by fitting the sun and angular sky radiance at four wavelengths (440, 675, 870, 1020 nm) to radiative transfer calculations (Dubovik and King, 2000).

ACPD
11, 7291–7319, 2011

Numerous studies have used AERONET data, owing to its high accuracy and easy access, for the validation of satellite-based aerosol inversions. In this study, we use AERONET-derived Level 2.0 (cloud-screened and quality assured) τ and SSA for the evaluation of OMAERUV aerosol retrieval over South America, central Africa and northern India.

3 Evaluation of OMAERUV aerosol optical depth over South America

3.1 Comparison of standard OMAERUV aerosol product to AERONET

A comparison of OMI-derived to AERONET-measured AOD's was carried out over a three-year period (2005–2007) at the seven AERONET sites in Table 1. OMAERUV aerosol retrievals are available at a spatial resolution of 13 by 24 km^2 at nadir, whereas AERONET are columnar point measurements. Therefore, it is important to formulate a correct method of co-location in order to compare spatial retrieval with point measurements. Due to larger pixel size of OMI, it is expected that a single closest OMI pixel will intercept reasonable area around AERONET sun-photometer site. Therefore, we use the closest OMI pixel to the sun-photometer site for comparison against AERONET. First, all the OMI aerosol retrieval in a given pass that fall within a grid box of size 0.5° by 0.5° centered at respective AERONET sites were extracted. Based on the radial distance from the AERONET site, a closest pixel was selected and co-located with the all AERONET measurements that fall within ±30 min of OMI overpass over that station. Thus, it is possible that a single OMI retrieval is co-located with more than one AERONET measurement which depends on the number of measurements available in given time window.

Figure 2 shows the comparison of collocated OMI AOD (y-axis) with that of AERONET (x-axis) for all seven stations over South America. OMI data with quality flag 0 and 1 are used in the comparison. Clearly, all OMI AOD retrieval with quality flag 1 and few with flag 0 are significantly over-estimated with respect to AERONET

ACPD
11, 7291–7319, 2011

measurements. Almost all retrievals with flag 1 fall outside the expected OMAERUV uncertainty range (0.1 or 30% whichever is larger). All flag 1 data in Fig. 2 that represent condition with AI > 1 and R_{388} up to 0.30, also represent high AOD condition (τ_{AERONET} up to 4 at 380 nm), whereas most flag 0 data points were confined to lower AOD regime ($\tau_{\text{AERONET}} < 1$ at 380 nm). Following the conditions defined for assigning flags, the current algorithm treats the most absorbing data (flag 1) as of lower quality in which only AAOD is considered to be reliable and not AOD. This is probably due to likely sub-pixel cloud contamination anticipated from the higher reflectivity at 388 nm. However, large values of AI strongly indicate the presence of absorbing aerosols over those pixels.

3.2 Causes of AERONET-OMI differences

The main source of uncertainty in the application of the near-UV technique to OMI observations is sub-pixel cloud contamination associated with the large size of the OMI footprint. The second most important source of uncertainty is the dependence on the assumed aerosol layer height. Other possible sources of error include surface albedo effects and aerosol model assumptions on particle size distribution and refractive index. The observed AOD over-estimations, however, are too large to be simply explained by sub-pixel cloud contamination, surface reflectance effects or assumed particle size distribution. The algorithm uses the minimum Lambertian surface reflectivity climatology database derived from TOMS instrument (1978–1993) (Herman and Celarier, 1997). The surface albedo in the UV region is low compared to that in the visible region and therefore, the error in the aerosol retrieval produced by the uncertainty associated with surface albedo is expected to be very low.

OMAERUV has to assume the aerosol vertical distribution for the retrieval. For smoke aerosol type over South America region, the algorithm assumes an aerosol vertical profile with Gaussian distribution with maximum concentration (peak) at 3 km. The Cloud-Aerosol Lidar and Infrared Pathfinder Satellite Observation (CALIPSO) satellite as a part of A-train constellation measures the vertical profile of back-scattered

ACPD
11, 7291–7319, 2011

radiation attenuated by clouds and aerosols over globe. The visual inspection of several CALIPSO overpass images available at http://www-calipso.larc.nasa.gov/ over biomass burning region show maximum back-scatter due to aerosols around 3 km height. For instance, for an aerosol event on 2 September 2007, OMAERUV algorithm derives a 388 nm AOD of 6 around Alta Floresta region with UV aerosol Index of 2.29, whereas AERONET measures AOD of 3.68 at about the same wavelength. The CALIPSO overpass show aerosol back-scatter peak around 3 km height over the same region on the same day. This suggests that the height of aerosols assumed by the OMI standard algorithm is likely to be correct and cannot explain the large over-estimation in OMI AOD retrieval.

The use of a gray aerosol optical model to represent the absorption properties of carbonaceous aerosol in the OMAERUV algorithm implies that black carbon is assumed to be the main aerosol component responsible for the satellite observed aerosol absorption of near-UV radiation. The spectral dependence of aerosol absorption optical depth is determined by the wavelength dependence of the imaginary refractive index. A parameter known as the Absorption Angstrom Exponent or AAE (Bond, 2001; Russell et al., 2010) is commonly used to describe the relative spectral dependence (RSD) of the aerosol absorption optical depth in a similar way that the Extinction Angstrom Exponent is used to describe the spectral dependence of the aerosol extinction optical depth. The AAE for the present OMI biomass burning aerosol models is close to black carbon or soot emitted from high-temperature combustion processes such as vehicle emission and urban/industrial aerosols whose wavelength-dependence of absorption can be approximated as $\lambda^{-1.0}$ in the UV-visible range (Bond, 2001; Bergstrom et al., 2002; Kline et al., 2004; Bond and Bergstrom, 2006). We will now examine the adequacy of the current implicit assumption on BC being the aerosol absorbing component driving the spectral dependence of the assumed aerosol model.

The relationship between AOD and the wavelength dependent imaginary refractive index was examined by a sensitivity analysis using radiative transfer calculations. Simulated radiances at 354 at 388 nm for several cases of spectrally dependent imaginary

ACPD
11, 7291–7319, 2011

refractive index and atmospheric aerosol load were used to calculate the corresponding Aerosol Index. Table 2 shows the corresponding AAE as a function of 388 nm imaginary refractive index and RSD of 0%, 20% and 30%. The spectral slope in aerosol absorption was achieved by increasing the imaginary refractive index at 354 nm while keeping it constant at 388 nm. The 0% RSD model yields AAE values of about 1, higher AAE values between about 2.5 and 3.0 are associated with the 20% RSD model, whereas even higher AAE values between 3.1 and 3.7 result from the 30% RSD assumption. The AI as a function of AOD was calculated for the three RSD assumptions in Table 2. In all three cases, AI increases monotonically with AOD, however, the magnitude of the AI increases as the RSD becomes larger. With the assumption of wavelength-dependent aerosol absorption, AI is found to be significantly higher than that computed with spectrally independent absorption for same values of AOD. This means that for a given observed value of AI, different RSD assumptions will result in as many distinct values of AOD. For instance, for an observed AI value of 2.0, the AOD derived assuming 30%, 20% and wavelength independent absorption would be about 0.55, 0.75, and 2.25, respectively. It means that with the assumption of "colored aerosols" (i.e., spectrally dependent absorption), the OMI near-UV observations can be explained with lower AOD that the ones required if the gray aerosol assumption is used. The result of this analysis suggests that the OMI near-UV retrieval of AOD is highly sensitive to the assumption about spectral aerosol absorption. The current assumption of wavelength-independent absorption which produces a large positive bias in the retrieval of AOD appears to be inappropriate.

4 Ground-based evidences of the spectral dependence in absorption

There have been increasing numbers of studies published in the recent years that report the in-situ and ground-based measurements of spectral aerosol absorption. Kirchstetter et al. (2004) have demonstrated the role of OC in the light absorption in biomass burning samples collected during SAFARI 2000. Their measurements showed that the

ACPD
11, 7291–7319, 2011

incomplete combustion process such as biomass burning can produce light-absorbing aerosols that have stronger spectral dependence in absorption, approximately $\lambda^{-2.0}$. As a result, OC in addition to BC contained in the biomass burning smoke contribute significantly to light absorption in the UV as well as at visible wavelengths. Hoffer et al. (2006) have reported the absorption angstrom exponent as high as 6–7 in the visible to UV range for the humic-like substances (HULIS) isolated from the biomass burning aerosol samples collected over the Amazon basin during LBA-SMOCC. Due to steep increase in the specific absorption from visible to UV, HULIS contribute up to 50% to the total light absorption at 300 nm and 20–30% between 350–400 nm. The later is relevant wavelength range to OMI aerosol sensing. Though, HULIS are weak absorber compared to the black carbon (BC) in the visible range, its relative contribution to the light absorption in UV-visible is non-negligible (8–11%). These results have significant importance in the photochemical processes and the UV remote sensing such as done by OMI.

A field campaign on the measurements of the columnar aerosol absorption at UV wavelengths using ground-based UV Multi-filter Rotating Shadowband Radiometer (UV-MFRSR) over Bolivia region in South America was conducted during an intense biomass burning season of September 2007 (N. Krotkov, personal communication). The direct sun and diffuse sky measurements are used to derive columnar single-scattering albedo and aerosol absorption optical depth (τ_{abs}). Their findings show that the both SSA and AAOD exhibit spectral dependence in the UV region where the absorption at 354 nm was greater than that at 388 nm. They report the wavelength dependence derived from spectral τ_{abs} measurements lies between $\lambda^{-2.0\,\text{to}\,-3.0}$ which is close to the range of AAE exhibited by the smoke aerosol model with 20% RSD in absorption.

In their recent work, Martins et al. (2009) have measured the spectral absorption efficiency of aerosol samples collected at Sao Paulo, Brazil. The selected Sao Paulo samples showed enhanced absorption at UV wavelengths which could result in 22% and 50% extra reduction in downward UV flux at 350 and 300 nm, respectively, at

ACPD
11, 7291–7319, 2011

surface. In a recent publication, Russell et al. (2010) used AERONET-derived columnar absorption aerosol optical depth (in the range 440–1020 nm) to deduce the AAE over several sites that are representative of different aerosol types. They highlight that the AAE is a strong indicator of type of aerosols since the wavelength dependence of aerosols is strongly influenced by their chemical and size composition. They found that the AAE values are near 1 for aerosol dominated by urban-industrial aerosols (largely contain black carbon), with larger values of AAE for biomass burning, and highest AAE values for Saharan dust aerosols. The AAE in the range 440–670 nm was ~1.5 for the Amazonian forest and South American Cerrado, which are the regions of interest in the present study.

5 New OMAERUV aerosol retrieval with assumption of wavelength-dependent absorption

5.1 AOD comparison

As demonstrated in Sect. 3, an increase in the assumed RSD of aerosol absorption in the forward calculations, would reduce the magnitude of retrieved AOD and thus may reduce the observed large bias between the satellite derived and the ground-based observations. Based on the theoretical calculations and on the limited observational basis discussed in Sect. 4 we can expect that the 20% RSD which is associated with AAE in the range 2.5 ~ 3.0 in OMI aerosol models is a more reasonable assumption that the current one. A set of look-up tables was created in which the pre-determined 354–388 nm spectral slope of the imaginary refractive index was changed from none (typical assumption for BC) to one in which the 354 imaginary refractive increases by 20% over the assumed value at 388 nm. Using a research version of the OMAERUV algorithm a new set of retrieval was carried out.

Figure 4 compares the new OMI retrieval of AOD at 388 nm with the ground-based observations at the AERONET sites used in the study. Unlike the original comparison

ACPD
11, 7291–7319, 2011

(Fig. 2), the new comparative analysis shows remarkably good agreement between OMAERUV results and AERONET measurements. The improvement is vast (~100%) for the previously labeled flag 1 where the new AOD is much better aligned with the ground-truth. About 60% of retrievals with quality flag 1 which are associated with higher reflectivity and enhanced AI now fall within the pre-estimated uncertainty against none in the standard OMI-AERONET comparison (see Fig. 2). The remaining cases of OMAERUV AOD over-estimation in Fig. 2 are likely to be the result of either sub-pixel cloud contamination or smoke layers located above clouds. Note that little change in the retrieval accuracy of weakly or non-absorbing aerosol data (flag 0) has taken place. This is because the difference between the two look-up-tables, one generated using gray models and other using colored models, is non-significant at lower values of optical depths. This means that at lower aerosol load associated with small optical depth, the assumption of gray or colored aerosols does not make significant difference in terms of retrieval of AOD at near-UV wavelengths. However, at moderate to large aerosol loading (AOD at 388 nm > 1), when absorption becomes significant, the assumption of spectrally independent absorption fails. In this condition, the assumption of wavelength-dependent aerosol absorption in the near-UV region better explains the measurements done by OMI at 354 and 388 nm wavelengths.

The left panel of Fig. 5 shows the spatial distribution of monthly mean AOD (at 0.5° by 0.5° resolution) at 388 nm for September 2007 over South America. The monthly composite was computed from the current OMAERUV aerosol Level-2 retrieval with quality flag 0 and 1. Very high values of AOD (~6) over the central Amazonia region indicates intense loading of smoke which also extends in eastward as well as southward directions. Note that the spatial pattern of aerosols over the eastern side follows the topography of the Andes which acts as a barrier and does not allow smoke to travel further on the other side. The right panel of Fig. 5 shows the spatial distribution of new retrieval of AOD (388 nm). The new retrieval of AODs are significantly lower in magnitude than that of standard OMI product with similar spatial distribution.

ACPD
11, 7291–7319, 2011

5.2 SSA comparison

Figure 6 shows the comparison of OMI and AERONET retrieved SSA for both standard (gray) and new (colored) OMAERUV aerosol model assumptions. OMAERUV-retrieved values have been converted to 441 nm (by interpolation between OMI reported 388 and 500 nm values) to facilitate the comparison with AERONET observations. The interpolated SSA at 441 nm was found to be lower than that at 388 nm as expected. This assumption of black carbon and organics as dominant components of smoke models results in SSA spectra in which absorption increases from near-UV to visible to near-IR. This is also consistent with the findings of other ground-based observations (Russell et al., 2010). Seventy five percent of new OMAERUV retrievals agree within the estimated uncertainty of the AERONET inversion (±0.03) as opposed to 55% when using the standard assumption.

5.3 Performance of OMAERUV over the other regions

The effect of using the new carbonaceous aerosol models was examined in regions other than the Amazon Basin. Biomass burning is a major anthropogenic source of gaseous and particulate matter over the southern African region (Formenti et al., 2003; Eck et al., 2003). During the Southern African Regional Science Initiative (SAFARI)-2000 experiment, several geophysical parameters, including aerosol size and optical properties were measured and assessed for understanding their spatial distribution and for the validation of satellite retrieval. The African burning season starts in June at about 10S and persists up to August. An AERONET sunphotometer installed at Mongu (−15.254° S, 23.151° E) provides longer record (from 1995 to 2007) of aerosol properties. The other region of interest is the northern India, the Indo-Gangetic Plane (IGP) in particular, where the biomass burning is known to be a major source of atmospheric load during winter (October–January) (Jethva et al., 2005, 2007). This region is unique in terms of its surrounding Himalayan topography, weather pattern, and aerosol seasonality. The multiyear aerosol data from AERONET sunphotometer

ACPD
11, 7291–7319, 2011

at Kanpur (26.45° N, 80.35° E) show that the aerosol optical depth (at 500 nm) ranges between 0.5–0.8 during winter months which are associated with relatively larger Extinction Angstrom Exponent (EAE > 1). In addition to the local sources, transported aerosols from other parts of this region also influence the aerosol properties measured by AERONET at Kanpur. MODIS-derived fine mode fraction and TOMS's aerosol index show widespread and persistence layer of smoke during winter over the region. Due to the influence of biomass burning aerosols and availability of good quality AERONET data, the Mongu and Kanpur AERONET sites, serve as a good test bed for evaluating the current and new assumption on the spectral aerosol absorption made in the OMI aerosol retrieval.

Figure 7 compares the co-located AOD derived by the standard (cross) and new (circle) OMAERUV algorithm with AERONET at Mongu and Kanpur. Here, only the satellite retrievals for which the current OMI algorithm identifies aerosol type as smoke were compared with AERONET. Clearly, AOD retrievals with the assumption of wavelength-dependent absorption (circle) are better aligned with those of AERONET. The root-mean-square error and percentage pixel that fall within the expected uncertainty improve significantly. While the RMS changes from 0.70 to 0.25, percentage pixels falling within uncertainty goes up from 40% to 77%. The improvement in the retrieval AOD at Kanpur and Mongu was observed mainly during month of October and August respectively. While largest improvement in AOD retrieval is obtained at larger values, a little effect is observed at lower values of optical depth. This is consistent with the OMI-AERONET comparison observed in the case of South America's biomass burning sites.

6 Conclusions

OMI instrument onboard NASA's AURA satellite derives the columnar total aerosol optical depth and single-scattering albedo (hence absorption optical depth) simultaneously at near-UV wavelengths operationally over the globe. Particularly, the retrieval

ACPD
11, 7291–7319, 2011

of later two are of greater importance in climate change as the sign of the aerosol radiative forcing (cooling or heating) depends on the aerosol absorption. However, we need to assess the accuracy of space-based inversion of aerosol parameters as these retrievals are carried out based on major assumptions about the state of atmosphere (aerosol properties) and surface. In this paper, we attempted to evaluate OMAERUV products of AOD and SSA against the equivalent measurements made by AERONET over biomass burning region of South America, central Africa, and northern India. The current version of OMI aerosol algorithm tended to over-estimate AOD significantly at near-UV wavelengths at higher aerosol loading (AOD at 388 nm > 1), when absorption at UV wavelengths also become large as evident from the high aerosol index. The standard OMAERUV algorithm assumes no spectral dependence in absorption between 354 and 388 nm for biomass burning aerosols. Driven by the theoretical calculations and ground-based evidence on the spectral aerosol absorption (or AAE), a fresh set of aerosol parameters were retrieved from OMI measurements with the assumed wavelength dependent absorption that follows $\lambda^{-2.5\,\text{to}\,-3.0}$ between 354 and 388 nm. The new retrievals of AOD were found to be in much better agreement with those of AERONET over selected sites. A large improvement in the retrieval of AOD occurs for measurements with higher reflectivity which is associated with large aerosol load and enhanced AI, therefore should be considered as good quality data. In addition, the single-scattering albedo at 388 nm was also retrieved with better accuracy. This paper strongly suggests that there clearly is a need to incorporate spectral dependence of absorption at UV wavelengths, which accounts the presence of organic carbon in the biomass burning aerosols, in the future version of OMAERUV aerosol products in order to retrieve more accurate aerosol extinction and absorption properties.

The use of limited ground-based information on the spectral dependence of aerosol absorption and a vast improvement in the retrieval of AOD and SSA at near-UV wavelengths from OMI measurements over smoke-dominated regions of South America, central Africa and northern India, suggest that the assumed wavelength-dependent aerosol absorption in the near-UV region ($\lambda^{-2.5\,\text{to}\,-3.0}$) is applicable to the major regions

ACPD
11, 7291–7319, 2011

of biomass burning analyzed here. The present study is probably the first satellite-based assessment that provides evidence on the strong wavelength-dependent absorption in the near-UV region, which is a proxy for the presence of organic aerosols, through OMI-AERONET comparison. Since the spectral signature of absorption by aerosol dominated by organic carbon ($\lambda^{-2.5\,\text{to}\,-3}$) differs significantly than that of black carbon ($\lambda^{-1.0}$), the spectral aerosol absorption quantified as AAE as inferred from OMI and other ground-based studies can be used as a potential indicator of relative dominance of OC and BC in total carbonaceous aerosols.

In addition to suggesting vast improvement in the retrieval of aerosol properties from OMI, present study also demonstrates, perhaps more importantly, the near-UV capabilities of OMI to identify organic carbon from pure black carbon in aerosol-laden region. When increasing number of studies demonstrates the association between aerosol type and its spectral aerosol absorption signature (or AAE), the near-UV inference of spectral absorption through the integration of OMI-AERONET measurements can be explored in detail for the identification of aerosol composition. This assumes importance in atmospheric chemistry, aerosol remote sensing, as well as aerosol-forced climate change.

Acknowledgements. We thank NASA's GES-DISC and OMI aerosol research team for their free online support of OMI/OMAERUV aerosol database. We also thank Brent Holben and other co-PI for establishing and maintaining AERONET sites whose data was used in this study.

References

Ahn, C., Torres, O., and Bhartia, P. K.: Comparison of Ozone Monitoring Instrument UV aerosol products with Aqua/Moderate Resolution Imaging Spectroradiometer and Multiangle Imaging Spectroradiometer observations in 2006, J. Geophys. Res., 113, D16S27, doi:10.1029/2007JD008832, 2008.

Bergstrom, R. W., Russell, P. B., and Hignett, P.: Wavelength dependence of the absorption

ACPD
11, 7291–7319, 2011

of black carbon particles: Predictions and results from the TARFOX experiment and implications for the aerosol single scattering albedo, J. Atmos. Sci., 59, 567–577, 2002.
Bond, T.: Spectral dependence of visible light absorption by carbonaceous particles emitted from coal combustion, Geophys. Res. Lett., 28, 4075–4078, 2001.
Bond, T. C. and Bergstrom, R. W.: Light absorption by carbonaceous particles: An investigative review, Aerosol Sci. Tech., 40, 27–67, 2006.
Dubovik, O. and King, M.: A flexible inversion algorithm for retrieval of aerosol optical properties from sun and sky radiance measurements, J. Geophys. Res., 105, 20673–20696, 2000.
Eck, T. F., Holben, B. N., Slutsker, I., and Setzer, A.: Measurements of irradiance attenuation and estimation of aerosol single scattering albedo for biomass burning aerosols in Amazonia, J. Geophys. Res., 103, 31865–31878, 1998.
Eck, T. F., Ward, D. E., Mukelabai, M. M., Dubovik, O., Smirnov, A., Schafer, J. S., Hsu, N. C., Piketh, S. J., Queface, A., Le Roux, J., Swap, R. J., and Slutsker, I.: Variability of biomass burning aerosol optical characteristics in southern Africa during the SAFARI 2000 dry season campaign and a comparison of single scattering albedo estimates from radiometric measurements, J. Geophys. Res., 108, 8477, doi:10.1029/2002JD002321, 2003.
Formenti, P., Elbert, W., Maenhaut, W., Haywood, J., Osborne, S., and Andreae, M. O.: Inorganic and carbonaceous aerosols during the Southern African Regional Science Initiative (SAFARI 2000) experiment: Chemical characteristics, physical properties, and emission data for smoke from African biomass burning, J. Geophys. Res., 108, 8488, doi:10.1029/2002JD002408, 2003.
Herman, J. R. and Celarier, E.: Earth surface reflectivity climatology at 340 and 380 nm from TOMS data, J. Geophys. Res., 102, 12059–12076, 1997.
Hoffer, A., Gelencsér, A., Guyon, P., Kiss, G., Schmid, O., Frank, G. P., Artaxo, P., and Andreae, M. O.: Optical properties of humic-like substances (HULIS) in biomass-burning aerosols, Atmos. Chem. Phys., 6, 3563–3570, doi:10.5194/acp-6-3563-2006, 2006.
Holben, B. N., Eck, T., Slutsker, I., Tanre', D., Buis, J. P., Setzer, A., Vermote, E., Reagon, J. A., Kaufman, Y. J., Nakajima, T., Lavenu, F., Jankowiak, I., and Smirnov, A.: AERONET-A federated instrument network and data archive for aerosol characterization, Rem. Sens. Environ., 66, 1–16, 1998.
Jethva, H., Satheesh, S. K., and Srinivasan, J.: Seasonal variability of aerosols over the Indo-Gangetic basin, J. Geophys. Res., 110, D21204, doi:10.1029/2005JD005938, 2005.
Jethva, H., Satheesh, S. K., and Srinivasan, J.: Evaluation of Moderate-Resolution Imag-

ACPD
11, 7291–7319, 2011

ing Spectroradiometer (MODIS) Collection 004 (C004) aerosol retrievals at Kanpur, Indo-Gangetic Basin, J. Geophys. Res., 112, D14216, doi:10.1029/2006JD007929, 2007.
Kahn, A. R., Gaitley, B. J., Martonchik, J. V., Diner, D. J., and Crean, K. A.: Multiangle Imaging Spectroradiometer (MISR) global aerosol optical depth validation based on 2 years of coincident Aerosol Robotic Network (AERONET) observations, J. Geophys. Res., 110, D10S04, doi:10.1029/2004JD004706, 2005.
Kaufman, Y. J., Tanré, D., Remer, L. A., Vermote, E. F., Chu, A., and Holben, B. N.: Operational remote sensing of tropospheric aerosol over the land from EOS-MODIS, J. Geophys. Res., 102, 17051–17067, 1997.
Kirchstetter, T. W., Novakov, T., and Hobbs, P. V.: Evidence that the spectral dependence of light absorption by aerosols is affected by organic carbon, J. Geophys. Res., 109, D21208, doi:10/1029/2004JD004999, 2004.
Kline, J., Huebert, B., Howell, S., Blomquist, B., Zhuang, J., Bertram, T., and Carrilo, J.: Aerosol composition and size versus altitude measured from the C-130 during ACE-Asia, J. Geophys. Res., 109, D19S08, doi:10.1029/2004JD004540, 2004.
Levelt, P. F., Hilsenrath, E., Leppelmeier, G. W., van den Ooord, G. H. J., Bhartia, P. K., Tamminen, J., de Haan, J. F., and Veefkind, J. P.: Science objectives of the Ozone Monitoring Instrument, IEEE Trans. Geosci. Remote Sens., 44(5), 1093–1101, 2006.
Levy, R. C., Remer, L. A., Mattoo, S., Vermote, E., and Kaufman, Y. J.: Second generation algorithm for retrieving aerosol properties over land from MODIS spectral reflectance, J. Geophys. Res., 112, D13211, doi:10.1029/2006JD007811, 2007.
Martins, J. V., Artaxo, P., Liousse, C., Reid, J. S., and Hobbs, P. V.: Effects of black carbon content, particle size and mixing on light absorption by aerosol particles from biomass burning in Brazil, J. Geophys. Res., 103, 32041–32050, 1998.
Martins, J. V., Artaxo, P., Kaufman, Y. J., Castanho, A. D., and Remer, L. A.: Spectral absorption properties of aerosol particles from 350–2500 nm, Geophys. Res. Lett., 36, L13810, doi:10.1029/2009GL037435, 2009.
Reid, J. S., Hobbs, P. V., Ferek, R. J., Blake, D. R., Martins, J. V., Dunlap, M. R., and Liousse, C.: Physical, chemical, and optical properties of regional hazes dominated by smoke in Brazil, J. Geophys. Res., 103, 32059–32080, 1998.
Remer, L. A., Kaufman, Y. J., Tanré, D., Mattoo, S., Chu, D. A., Martins, J. V., Li, R. R., Ichoku, C., Levy, R. C., Kleidman, R. G., Eck, T. F., Vermote, E., and Holben, B. N.: The MODIS algorithm, products and validation, J. Atmos. Sci., 62, 947–973, 2005.

ACPD
11, 7291–7319, 2011

Russell, P. B., Bergstrom, R. W., Shinozuka, Y., Clarke, A. D., DeCarlo, P. F., Jimenez, J. L., Livingston, J. M., Redemann, J., Dubovik, O., and Strawa, A.: Absorption Angstrom Exponent in AERONET and related data as an indicator of aerosol composition, Atmos. Chem. Phys., 10, 1155–1169, doi:10.5194/acp-10-1155-2010, 2010.

Torres, O., Bhartia, P. K., Herman, J. R., Ahmad, Z., and Gleason, J.: Derivation of aerosol properties from satellite measurements of backscattered ultraviolet radiation: Theoretical basis, J. Geophys. Res., 103, 17099–17110, 1998.

Torres, O., Bhartia, P. K., Herman, J. R., Sinyuk, A., Ginoux, P., and Holben, B.: A long-term Record of aerosol optical depth from TOMS observations and comparison to AERONET measurements, J. Atmos. Sci., 59, 398–413, 2002.

Torres, O., Tanskanen, A., Veihelmann, B., Ahn, C., Braak, R., Bhartia, P. K., Veefkind, P., and Levelt, P.: Aerosols and surface UV products from Ozone Monitoring Instrument observations: An overview, J. Geophys. Res., 112, D24S47, doi:10.1029/2007JD008809, 2007.

Torres, O., Chen, Z., Jethva, H., Ahn, C., Freitas, S. R., and Bhartia, P. K.: OMI and MODIS observations of the anomalous 2008–2009 Southern Hemisphere biomass burning seasons, Atmos. Chem. Phys., 10, 3505–3513, doi:10.5194/acp-10-3505-2010, 2010.

Venkataraman, C., Habib, G., Eiguren-Fernandez, A., Miguel, A. H., and Friedlander, S. K.: Residential biofuels in south Asia: Carbonaceous aerosol emissions and climate impacts, Science, 307, 1454–1456, 2005.

Zhang, Y., Fu, R., Yu, H., Qian, Y., Dickinson, R., Dias, M. A. F. S., da Silva Dias, P. L., and Fernandes, K.: Impact of biomass burning aerosol on the monsoon circulation transition over Amazonia, Geophys. Res. Lett., 36, L10814, doi:10.1029/2009GL037180, 2009.

ACPD
11, 7291–7319, 2011

Table 1. Geolocation data and mean aerosol optical depth (500 nm) during biomass burning season (August–September) over AERONET stations in South America.

Station name	Latitude	Longitude	Elevation (in meters)	Data period	Mean AERONET AOD (500 nm)
Alta Floresta	−9.871	−56.104	277	Oct 2004–Dec 2007	0.93
Rio Branco	−9.957	−67.869	212	Oct 2004–Feb 2008	0.95
Ji Parana	−10.934	−62.852	218	Jun 2006–Sep 2008	0.74
Cuiaba Miranda	−15.729	−56.021	210	Oct 2004–Nov 2007	0.73
Santa Cruz Utepsa	−17.767	−63.201	432	Sep 2006–Oct 2007	0.80
Santa Cruz	−17.802	−63.178	442	Oct 2004–Mar 2006	0.68
Campo Grande Sonda	−20.438	−54.538	677	Oct 2004–Sep 2008	0.34

ACPD
11, 7291–7319, 2011

Table 2. The imaginary component of refractive index and associated absorption angstrom exponent (α_{abs}) for nil, 20% and 30% spectral dependence between 354 and 388 nm.

No spectral dependence		20% spectral dependence		30% spectral dependence	
Img. Ref. Index 388/354	α_{abs}	Img. Ref. Index 388/354	α_{abs}	Img. Ref. Index 388/354	α_{abs}
0.048/0.048	1.01	0.048/0.0576	2.49	0.048/0.0624	3.12
0.040/0.040	1.03	0.040/0.0480	2.54	0.040/0.0520	3.20
0.030/0.030	1.06	0.030/0.036	2.62	0.030/0.0390	3.29
0.020/0.020	1.07	0.020/0.024	2.67	0.020/0.0260	3.37
0.010/0.010	1.11	0.010/0.012	2.84	0.010/0.0130	3.60
0.005/0.005	1.13	0.005/0.006	2.92	0.005/0.0650	3.70
0.000/0.000	N/A	N/A	N/A	N/A	N/A

ACPD
11, 7291–7319, 2011

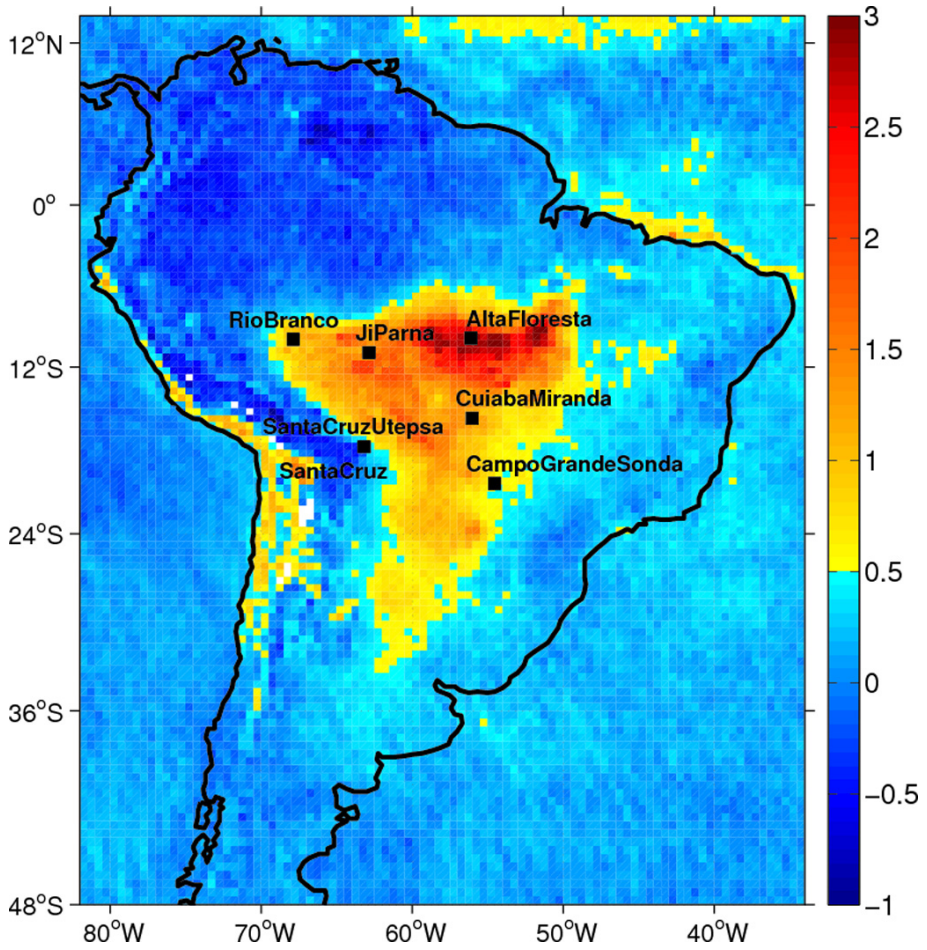

Fig. 1. Monthly mean UV aerosol index derived from OMI for September 2007 over South America. Depicted inside are locations of seven AERONET stations whose data was used in this study.

ACPD
11, 7291–7319, 2011

OMAERUV aerosol retrieval in biomass burning environment

H. Jethva and O. Torres

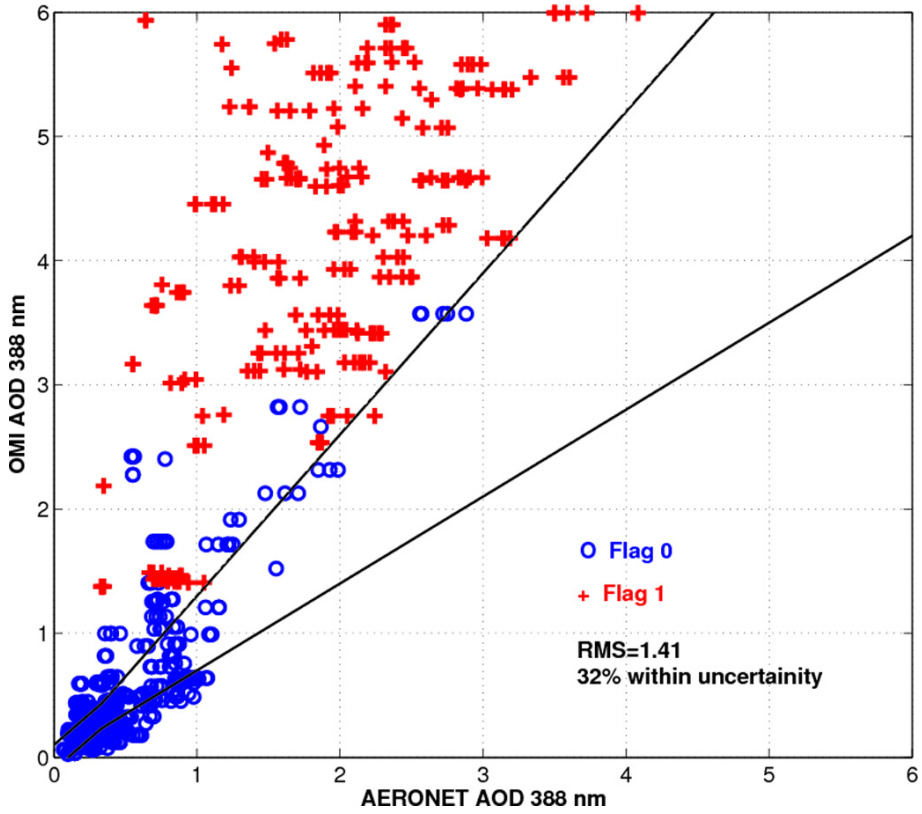

Fig. 2. Scatter-plot of co-located spectral aerosol optical depth between OMI (y-axis) and AERONET (x-axis) for seven stations over the biomass burning region of South America. OMI data with flag 0 (circle) and flag 1 (plus sign) were used in the comparison. The solid lines are pre-calculated uncertainty in OMI AOD retrieval.

ACPD
11, 7291–7319, 2011

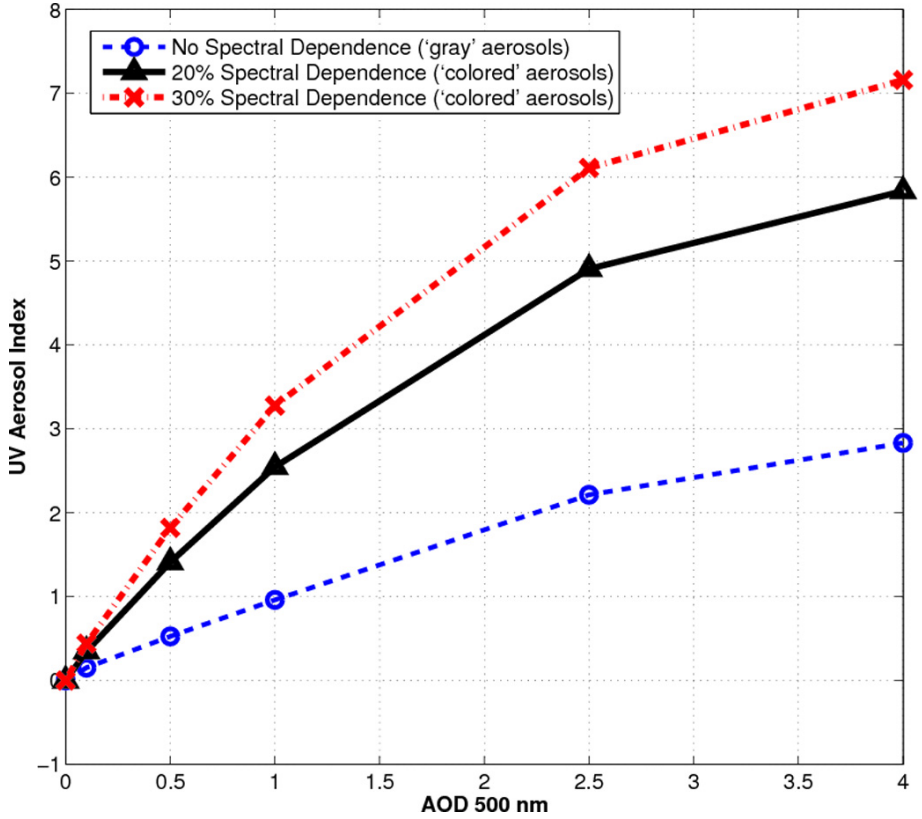

Fig. 3. UV Aerosol Index as a function of aerosol optical depth for varying spectral absorption in the range 354–388 nm.

ACPD
11, 7291–7319, 2011

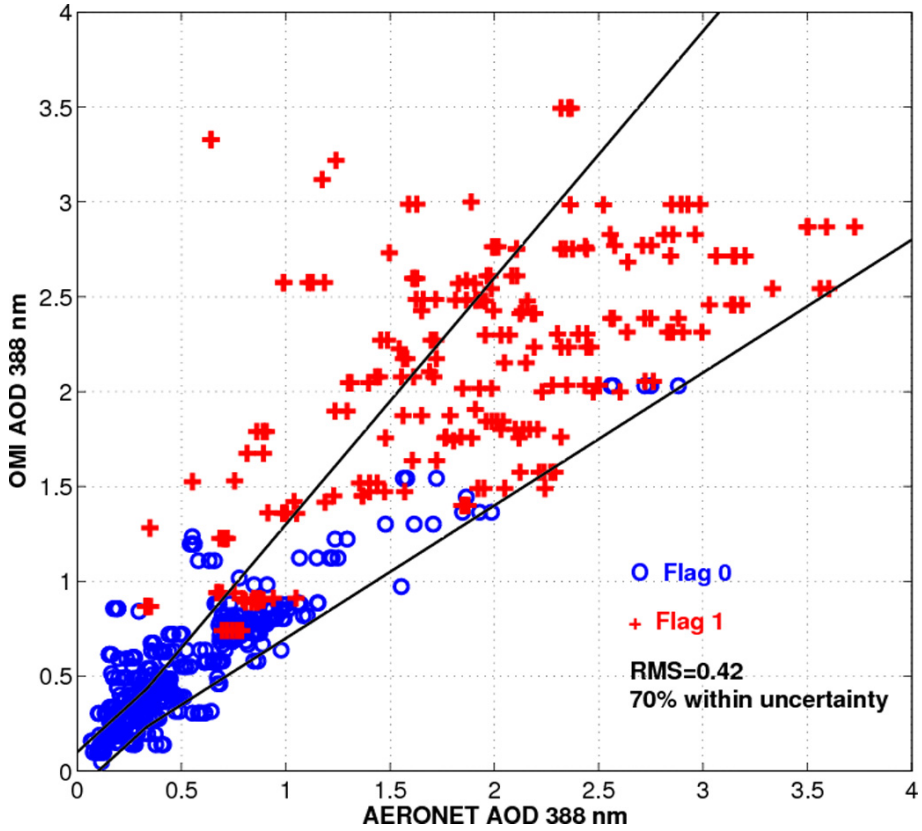

Fig. 4. Comparison of the new OMI retrieval of aerosol optical depth (y-axis) with that of AERONET (x-axis) at 388 nm for the biomass burning region of South America. OMI data with flag 0 (circle) and flag 1 (plus sign) were used in the comparison. The solid lines are pre-calculated uncertainty in OMI AOD retrieval.

ACPD
11, 7291–7319, 2011

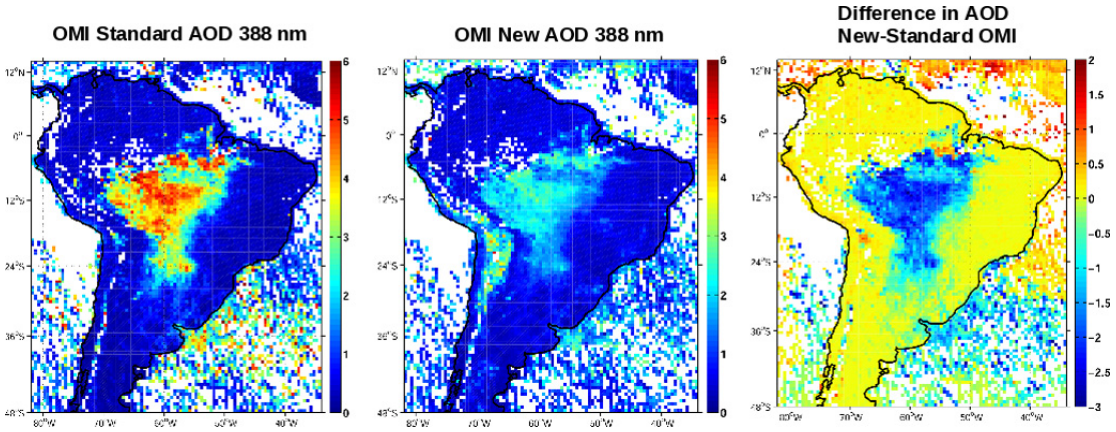

Fig. 5. Spatial distribution of monthly mean aerosol optical depth for September 2007 derived from the standard OMAERUV aerosol product (left panel) and new proposed retrieval (middle panel). The absolute difference between them is shown in right panel. All three distributions are at 0.5° by 0.5° resolution.

ACPD
11, 7291–7319, 2011

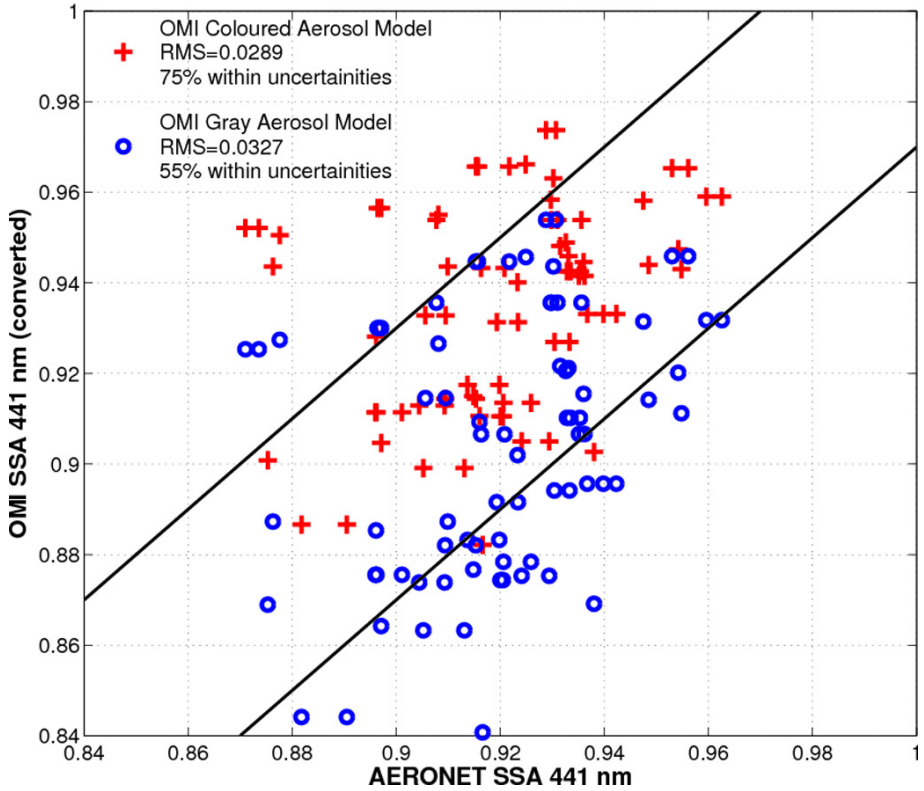

Fig. 6. Comparison of single-scattering albedo at 441 nm derived by OMI standard (circle) and new aerosol models (plus sign) with that of AERONET inversion over biomass burning sites in South America for the period 2004–2008. Dashed lines are uncertainty of $\Delta\omega = \pm 0.03$ in the AERONET inversion.

ACPD
11, 7291–7319, 2011

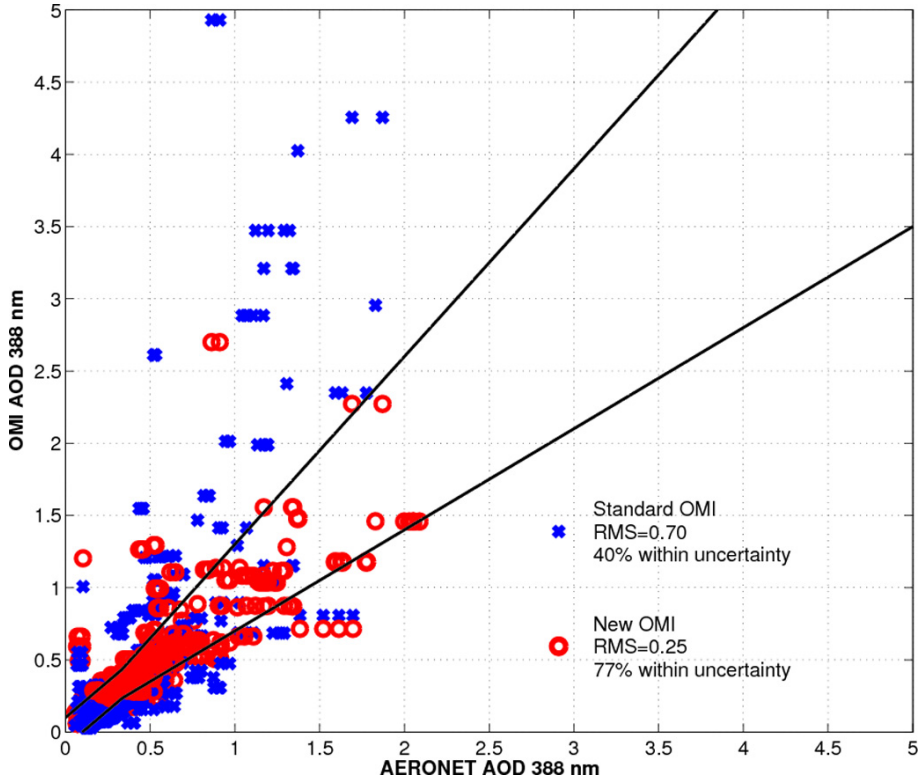

Fig. 7. Scatter-plot of smoke aerosol optical depth at 388 nm derived by standard (cross) and new (circle) OMI aerosol algorithm and AERONET for Mongu (−15.254° S, 23.151° E) and Kanpur (26.45° N, 80.35° E) for the period 2004–2008.

ACPD
11, 7291–7319, 2011